Polyamide 6/maleated Ethylene–propylene–diene Rubber/organoclay Composites with or Without glycidyl Methacrylate as a Compatibilizer

Lingyan Zhang, Chaoying Wan, Yong Zhang

State Key Laboratory of Metal Matrix Composites, School of Chemistry and Chemical Technology, Shanghai Jiao Tong University, Shanghai 200240, China

Received 26 January 2008; accepted 23 May 2008
DOI 10.1002/app.28768
Published online 30 July 2008 in Wiley InterScience (www.interscience.wiley.com).

ABSTRACT: Polyamide 6 (PA6)/maleated ethylene–propylene–diene rubber (EPDM-*g*-MA)/organoclay (OMMT) composites were melt-compounded through two blending sequences. Glycidyl methacrylate (GMA) was used as a compatibilizer for the ternary composites. The composite prepared through via the premixing of PA6 with OMMT and then further melt blending with EPDM-*g*-MA exhibited higher impact strength than the composite prepared through the simultaneous blending of all the components. However, satisfactorily balanced mechanical properties could be achieved by the addition of GMA through a one-step blending sequence. The addition of GMA improved the compatibility between PA6 and EPDM-*g*-MA, and this was due to the reactions between PA6, EPDM-*g*-MA, and GMA, as proved by Fourier transform infrared analysis and solubility (Molau) testing. In addition, OMMT acted as a compatibilizer for PA6/EPDM-*g*-MA blends at low contents, but it weakened the interfacial interactions between PA6 and EPDM-*g*-MA at high contents. Both OMMT and GMA retarded the crystallization of PA6. The complex viscosity, storage modulus, and loss modulus of the composites were obviously affected by the addition of OMMT and GMA. J Appl Polym Sci 110: 1870–1879, 2008

Key words: compatibilization; nanocomposites; organoclay; polyamides; rubber

INTRODUCTION

The toughening of polyamides (PAs) can be achieved through melt blending with functionalized elastomers.[1–4] Both the dispersed phase size and interparticle distance play important roles in governing the level of toughening. It has been reported that the rubber particle size should be controlled in the range of 0.1–1 μm and that the interparticle distance should be below the critical interparticle distance to attain supertough PA materials.[1,2] However, incorporating a low-modulus elastomer into PA usually leads to a reduction of the stiffness and strength. To prepare high-performance PA composites, a combination of elastomers and inorganic fillers (e.g., nanoclay) to modify PA has attracted significant academic and industrial interest.[5–16]

Recently, many research groups have reported that PA/maleated elastomer/organoclay (OMMT) composites display satisfactorily balanced mechanical properties.[8–16] For example, a polyamide 6 (PA6)/maleated styrene–ethylene–butylene–styrene (SEBS-*g*-MA; 70/30) blend with 3 wt % OMMT exhibited supertough behavior along with a 44% increase in the modulus in comparison with a PA6/SEBS-*g*-MA (70/30) blend.[14] Furthermore, the toughness of PA/maleated elastomer/OMMT composites is significantly influenced by the blending sequences.[8,10,13] Blending an elastomer with a premixed PA6/OMMT nanocomposite can lead to a higher notched impact strength than the other two blending methods, that is, blending an elastomer, PA, and OMMT simultaneously and blending a PA/maleated elastomer blend with OMMT; this is because the sequence favors the maximum amount of OMMT in the PA matrix in comparison with other blending sequences.[8,10,13] However, this two-step blending sequence (N2) costs more and is time-consuming from the point of view of industry. Therefore, it is necessary to develop a new method to produce high-performance PA/elastomer/OMMT ternary composites by a one-step blending sequence (N1).

For PA/maleated elastomer blends, the maleic anhydride group can readily react with the amine end group of PA to form a grafted copolymer that strengthens the interfacial adhesion between the two phases, leading to a supertough material.[1–4] Moreover, the toughness of such blends can be further

Correspondence to: Y. Zhang (yong_zhang@sjtu.edu.cn).
Contract grant sponsor: Shanghai Leading Academic Discipline Project; contract grant number: B202.

enhanced by the addition of functional monomers or polymers. For example, a multifunctional epoxy compound was added to PA6/maleated poly(ethylene octene) elastomer blends, and the notched impact strength significantly increased because of the coupling action of the epoxy compound.[17] Hyperbranched polymer-grafted maleated polypropylene was used to increase the elongation at break of PP/PA6 blends because of the improvement of the interfacial adhesion between PA6 and maleated polypropylene.[18]

The incorporation of OMMT into PA/maleated elastomer blends resulted in a significant reduction of the toughness, which was attributed to the poor interfacial adhesion and the blockage of the overlapping stress volume of the functionalized elastomer to a large extent in the presence of OMMT.[8–11,14–16] The improvement of the interfacial adhesion between PA6 and the elastomer could compensate for the toughness loss. The goal of this work was to propose an economical one-step blending approach to balancing the mechanical properties of PA6/functionalized elastomer/OMMT composites through the use of glycidyl methacrylate (GMA) as an interfacial modifier. The effects of OMMT and GMA on the mechanical properties, phase morphology, crystallization, and rheological behavior of PA6/maleated ethylene–propylene–diene copolymer (EPDM-*g*-MA)/OMMT composites were investigated.

EXPERIMENTAL

Materials

PA6 (8202NL) was produced and kindly supplied by Honeywell Co. (Morristown, NJ). EPDM-*g*-MA (CMG9802) with a 0.8% MA concentration was purchased from Shanghai Sunny New Technology Development Co. (Shanghai, China). OMMT (Nanomer I.30TC) was a commercial product from Nanocor, Inc. (Arlington Heights, IL). GMA was an industrial-grade product.

Specimen preparation

Before extrusion, PA6 and OMMT were dried in a vacuum oven at 80°C for 24 h, and EPDM-*g*-MA was vacuum-dried for 4 h at 60°C. All composites were prepared in a Berstoff corotating twin-screw extruder type ZE25, Berstoff Corp., Hanover, Germany, length/diameter ratio = 41, screw diameter = 25 mm. The barrel temperatures were kept at 220–240°C. The screw speed was fixed at 280 rpm. The extruded rods were cooled in a water bath, pelletized, and dried in an air oven at 80°C for 24 h. Injection molding was carried out in a plastic injection-molding machine (HTB110X/1, Ningbo Haitian Co., Jiangsu Province, China) to obtain tensile (thickness = 3.2 mm), flexural (thickness = 3.2 mm), and impact (thickness = 3.2 mm) specimens. Most PA6/EPDM-*g*-MA/OMMT ternary composites were prepared by N1, which means that PA6, EPDM-*g*-MA, OMMT, and GMA were blended simultaneously. The weight ratio of PA6 to EPDM-*g*-MA was kept at 80/20. The OMMT content was 1 or 4 phr, and the GMA content was 0 or 1 phr. *phr*, which is the abbreviation of parts per hundred parts of resin, means the weight percentage of the filler with respect to 100 units by weight of the polymer matrix; for example, in this study, the weight ratio for PA6/EPDM-*g*-MA/OMMT/GMA (4 phr OMMT and 1 phr GMA) was 80/20/4/1. In N2, PA6 was blended with OMMT (4 phr) initially, and then the composite was mixed with EPDM-*g*-MA. For comparison, pure PA6, PA6/OMMT (80/4), PA6/EPDM-*g*-MA (80/20), PA6/ethylene–propylene–diene rubber (EPDM)/GMA (80/20/1), and PA6/GMA (80/1) were prepared under the same melt-processing condition used for the ternary composites.

Characterization and testing

Tensile properties and flexural properties were measured with an Instron model 4465 apparatus (Instron Co., Canton, MA) according to ASTM D 638 and ASTM D 790, respectively. The notched Izod impact strength was determined with a V-shape notch on a Ray-Ran universal pendulum impact tester (Ray-Ran Test Equipment Ltd., Nuneaton, UK) according to ASTM D 256. An average value of five repeated tests was taken for each composition. Standard deviations were less than 2% for the yield strength, 20% for the elongation at break, 5% for the flexural modulus, 2% for the flexural strength, and 10% for the notched impact strength.

The fracture surfaces of the samples were observed by means of field emission scanning electron microscopy (FESEM; JSM-7401F, JEOL Ltd., Tokyo, Japan). Images were taken from cryogenically fractured surfaces of specimens. The fractured surfaces were etched with boiling toluene at the ambient temperature for 1 h to remove the elastomer phase and then coated with gold for observation. The photomicrographs of FESEM were analyzed with an image analyzer to determine the size of the dispersed phase. A minimum of 200 dispersed particles were considered on each fractograph to identify the size distribution. Weight-average rubber particle size ($\bar{d}_w$) values were calculated from the distribution of sizes with the following equation:

$$\bar{d}_w = \sum n_i d_i^2 \Big/ \sum n_i d_i$$

where n_i is the number of particles with diameter d_i.

TABLE I
Mechanical Properties of the PA6/EPDM-*g*-MA/OMMT Composites Prepared with Different Blending Sequences

		PA6/EPDM-*g*-MA/OMMT				
Property	GMA content (phr)	100/0/0	80/20/0	80/20/1 (N1)	80/20/4 (N1)	80/20/4 (N2)
Notched impact strength (J/m)	0	45	709	422	232	545
	1			581	406	
Elongation at break (%)	0	32	101	112	13	12
	1			170	23	
Yield strength (MPa)	0	70.4	45.6	52.7	57.0	57.8
	1			52.3	56.6	
Flexural strength (MPa)	0	94.9	61.4	68.6	80.6	79.1
	1			67.2	76.1	
Flexural modulus (MPa)	0	2301	1502	1760	2126	2153
	1			1682	2098	

A Molau test was conducted through the mixing of about 0.4 g of a sample with 10 mL of formic acid in a test tube.[19] The mixture was vigorously shaken and left alone for 30 days.

The Fourier transform infrared (FTIR) analysis was conducted on a PerkinElmer Paragon 1000 FTIR spectrometer (Perkin Elmer Inc., Wellesley, MA) in the scanning range of 4400–400 cm^{-1} with a resolution of 4 cm^{-1}. The insoluble component of the PA6/EPDM-*g*-MA/OMMT/GMA (80/20/4/1) composite after the Molau tests was filtered and washed several times with fresh formic acid and distilled water and then was dried overnight in a vacuum oven at 80°C. The dried sample was pressed into a thin film for testing.

The dynamic mechanical properties were measured with a rheometer (DMA 242C, Netzsch Inc., Bavaria, Germany) in a cantilever mode at a frequency of 1 Hz with a dynamic strain of 0.01% over a temperature range of −90 to 100°C at a heating rate of 3°C/min.

The PA6 crystal forms of the composites were characterized with a Rigaku (Tokyo, Japan) model D/max-2B diffraction meter. The X-ray beam was nickel-filtered Cu Kα ($\lambda = 0.154$ nm) radiation and was operated at 40 kV and 30 mA. Data were obtained from 1.1 to 35° (2θ) at a scanning rate of 4°/min.

The thermal properties of the samples were measured with a PerkinElmer differential scanning calorimeter. All tests were performed in a nitrogen atmosphere with a sample weight of about 6 mg. All samples were first heated from room temperature to 280°C at 20°C/min and kept there for 3 min to eliminate the previous thermal history. The specimen was subsequently cooled to 25°C at a cooling rate of 10°C/min and then heated again to 280°C at 10°C/min. The melting temperature (T_m) and melting enthalpy were determined in the second heating scan from the maximum temperature and the peak area, respectively. The crystallization temperature (T_c) was measured in the cooling scan. The crystallinity of PA6 was calculated under the assumption of a melting heat of 190.6 J/g for 100% crystalline PA6.[20]

Rotational rheological measurements were carried out in an oscillatory mode on a rheometer (Gemini 200 rheometer, Bohlin Co., Worcestershire, UK) equipped with a parallel-plate geometry using 25-mm-diameter plates at 240°C and a frequency range of 0.01–100 $rad \cdot s^{-1}$. The samples were 2.0 mm thick. The elastic modulus (G'), viscous modulus (G''), complex viscosity (η*), and ratio of the viscous force to the elastic force [or loss factor (tan δ)] were measured in the frequency sweep experiments.

RESULTS AND DISCUSSION

Mechanical properties

Table I shows the mechanical properties of PA6/EPDM-*g*-MA/OMMT composites, with or without GMA, prepared by two different blending sequences (N1 and N2). The PA6/EPDM-*g*-MA/OMMT ternary composites prepared by N1 had mechanical properties balanced between those of PA6 and PA6/EPDM-*g*-MA blends. The yield strength, flexural strength, and flexural modulus of the ternary composites (N1) obviously increased with increasing OMMT content, but the impact strength and elongation at break decreased dramatically. The ternary composites prepared via different methods (N1 and N2) showed a great difference in the notched impact strength, even for the same formulation. The notched impact strength of the one composite [80/20/4 (N2)] was 135% higher than that of the other composite [80/20/4 (N1)], and this means that the impact strength was influenced by the blending sequences. The ternary composite [80/20/4 (N2)] was produced through the premixing of PA6 and OMMT first and then melt blending with EPDM-*g*-MA. Most OMMT layers were located in the PA6 matrix through this procedure.[8,13–16] In comparison with N2, the other composite [80/20/4 (N1)] was prepared through the simultaneous melt blending of

all the components. The OMMT layers were dispersed in both phases.[8] The presence of OMMT in the EPDM-*g*-MA phase reduced its ability to cavitate, and this finally resulted in reduced toughening efficiency. Dasari et al.[8] reported the same phenomenon in polymide66/SEBS-*g*-MA/OMMT composites.

For the ternary composites prepared via method N1, the yield strength, flexural strength, and flexural modulus just slightly decreased after the addition of 1 phr GMA, whereas the impact strength and elongation at break were significantly enhanced, because the chemical reactions between PA6, EPDM-*g*-MA, and GMA could enhance the interfacial adhesion between PA6 and EPDM-*g*-MA rubber. Compared with the ternary composite prepared via N2, PA6/EPDM-*g*-MA/OMMT/GMA (80/20/4/1) prepared via N1 showed a higher elongation at break and similar flexural properties and yield strength. Thus, it is proposed that PA6/EPDM-*g*-MA/OMMT ternary composites with satisfactorily balanced mechanical properties can be achieved by N1 in the presence of GMA.

Morphology

The morphology of the ternary composites was characterized with FESEM, as shown in Figure 1. The holes and knobs on the fracture surface of the PA6 matrix reflected the morphology of the dispersed EPDM-*g*-MA phase. Figure 1(a–c) shows the morphology of the fracture surfaces of ternary composites with different OMMT contents. The average size ($\bar{d}_w$) of the dispersed EPDM-*g*-MA phase decreased from 0.23 to 0.21 μm after the addition of 1 phr OMMT (Table II) but increased to 0.24 μm with the addition of 4 phr OMMT. OMMT can enhance the compatibility of polymers because of the formation of *in situ* grafts[21] and can act as a barrier to prevent dispersed phase coalescence,[22] so the rubber particle size decreased at low clay loadings. With increasing OMMT content, OMMT weakened the interfacial adhesion between PA6 and EPDM-*g*-MA, leading to an increase in the rubber size and a decrease in the impact strength of the composites.[9] Figure 1(d–f) shows the morphology of the ternary composites with the addition of 1 phr GMA. For PA6/EPDM-*g*-MA (80/20), fewer holes were observed on the fracture surfaces of the samples, and the interfacial boundary between the rubber phase and matrix became rougher with the addition of GMA. For PA6/EPDM-*g*-MA/OMMT (80/20/4), the addition of GMA reduced $\bar{d}_w$ of the dispersed EPDM-*g*-MA phase from 0.24 to 0.22 μm (Table II). This indicates that GMA enhanced the interfacial adhesion between PA6 and EPDM-*g*-MA and acted as a compatibilizer in the composites.

Molau test and FTIR analysis

A Molau test was applied to confirm possible reactions between PA6, EPDM-*g*-MA, and GMA. The PA6/EPDM-*g*-MA (80/20) and PA6/EPDM-*g*-MA/OMMT (80/20/4) composites with and without GMA were extracted with formic acid, which is a good solvent for PA6 but not for EPDM-*g*-MA rubber. Figure 2 shows the results of the Molau test. A milky and colloidal suspension was observed for the PA6/EPDM-*g*-MA (80/20) composite, as shown in Figure 2(a), which was attributed to the emulsifying effect of the copolymer *in situ* formed during melt processing.[19] Figure 2(b) shows a milky suspension, similar to that shown in Figure 2(a), which persisted in the solution containing the PA6/EPDM-*g*-MA/OMMT (80/20/4) composites, and the upper part of the tube generated a few insoluble components. For the GMA-modified PA6/EPDM-*g*-MA/OMMT composite [see Figure 2(c)], phase separation was observed. The bottom part of the tube in Figure 2(c) presented a slightly milky solution, and the upper part of the tube showed a suspension that was composed of a large quantity of visible macroscopic particles insoluble in the formic acid. The insoluble fraction of PA6/EPDM-*g*-MA/OMMT/GMA and PA6/EPDM-*g*-MA/OMMT was probably due to the formation of a crosslinking network between PA6, EPDM-*g*-MA, and OMMT. Compared to PA6/EPDM-*g*-MA/OMMT, PA6/EPDM-*g*-MA/OMMT/GMA showed a much larger and more insoluble fraction and lower turbidity of the formic acid solvent, and this indicated that GMA could enhance the formation of a semi-interpenetrating network through the chemical reactions between PA6, EPDM-*g*-MA, and GMA. This conjecture is supported by the following FTIR analysis.

The possible reactions between PA6, EPDM-*g*-MA, and GMA were investigated by means of FTIR. Figure 3 shows the FTIR spectra of PA6, PA6/GMA, and GMA. GMA showed an absorption peak at 908 cm^{-1} that was attributed to the epoxy group. After the melt blending of GMA with PA6, this peak disappeared, and this indicated that a chemical reaction must have happened between GMA and PA6. The FTIR spectrum of the insoluble fraction of PA6/EPDM-*g*-MA/OMMT/GMA (80/20/4/1) in formic acid is shown in Figure 4. The stretching vibration peak of C=O of maleic anhydride at 1780 cm^{-1} was not observed, and this suggested that the carbonyl groups of maleic anhydride of EPDM-*g*-MA reacted with the functional group of PA6. The bands at 1082 and 1019 cm^{-1} were due to Si—O stretching of OMMT,[23] and this means that OMMT existed in the insoluble fraction. Besides the characteristic absorption peaks of —CH_2 and —CH_3 at 1236, 1375, and 720 cm^{-1},[24,25] the strong characteristic absorption peaks of PA6 at 3287, 3093, 1645, and 1539 cm^{-1} also

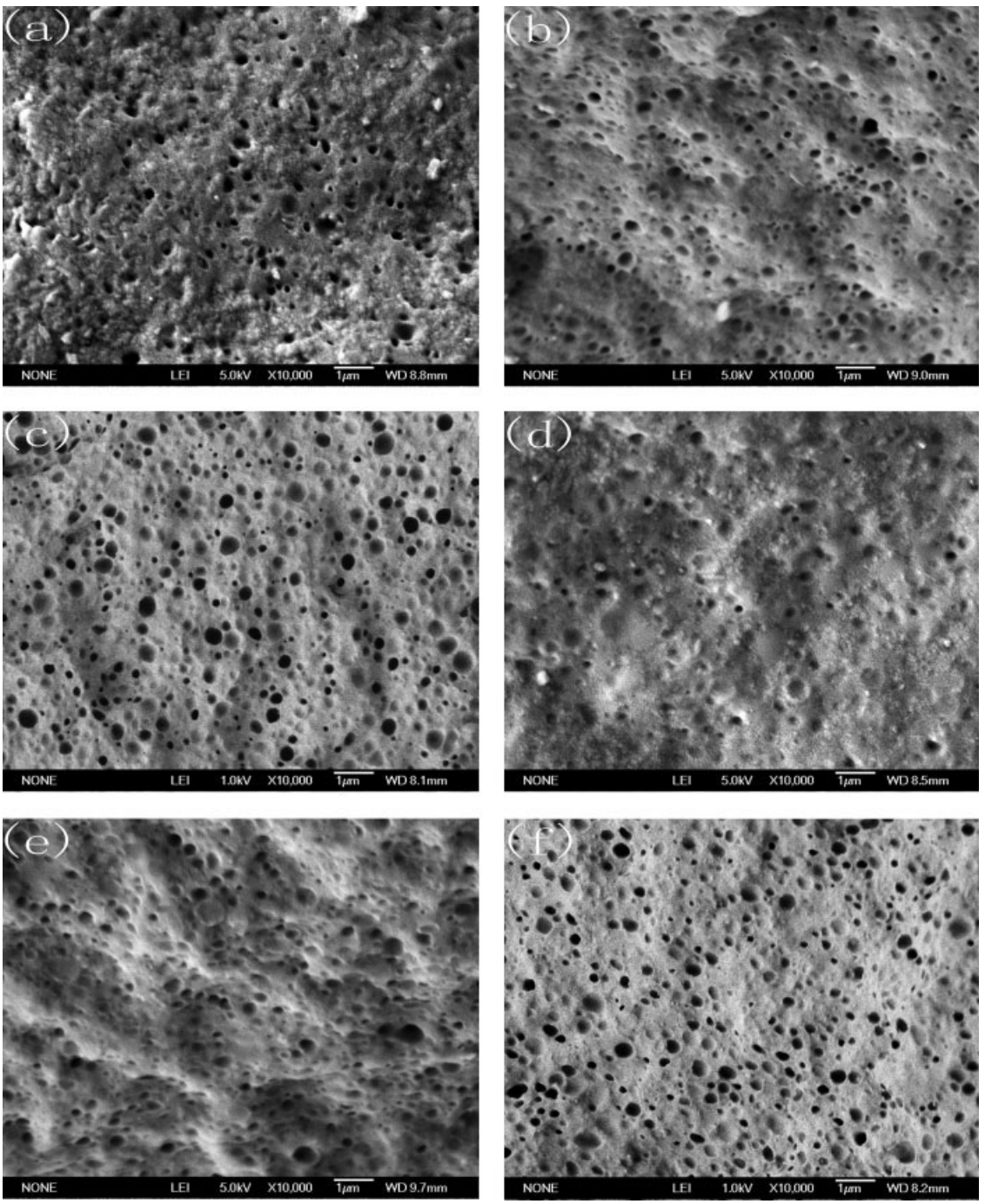

Figure 1 FESEM micrographs of the PA6 composites prepared by method N1 with PA6/EPDM-*g*-MA/OMMT/GMA compositions of (a) 80/20/0/0, (b) 80/20/1/0, (c) 80/20/4/0, (d) 80/20/0/1, (e) 80/20/1/1, and (f) 80/20/4/1.

appeared.[24,25] Hence, it is believed that the insoluble fraction consisted of PA6, EPDM-*g*-MA, and OMMT. Furthermore, the film used for FTIR testing was placed in 10 mL of a toluene solution at the ambient temperature and left alone for another 48 h. The film sank in toluene but was not dissolved, and this demonstrated that chemical reactions occurred between PA6, EPDM-*g*-MA, and GMA and formed a crosslinking network among all the components. A reaction mechanism is proposed in Scheme 1.

TABLE II
Dimensions of the Rubber Particles in the PA6 Composites Expressed as a Function of the OMMT Content (*x*) and GMA Content (*y*) in 80/20/*x*/*y* Compositions of PA6/EPDM-*g*-MA/OMMT/GMA

		$x = 0$	$x = 1$	$x = 4$
$\bar{d}_w$ (μm)	$y = 0$	0.23	0.21	0.24
	$y = 1$	0.23	0.22	0.22

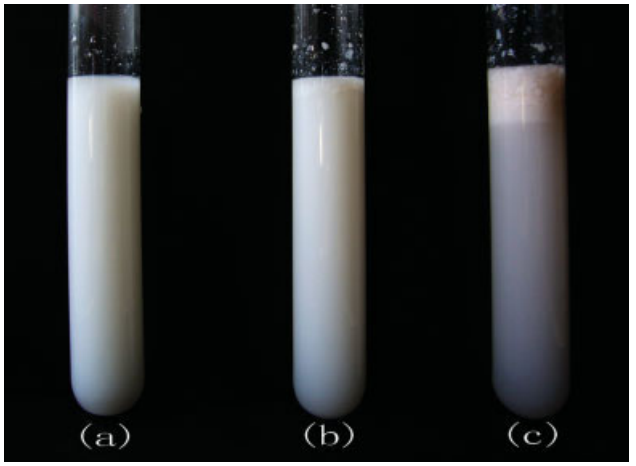

Figure 2 Picture of the test tubes used for the Molau tests carried out on the PA6/EPDM-*g*-MA/OMMT/GMA composites (prepared by method N1) with compositions of (a) 80/20/0/0, (b) 80/20/4/0, and (c) 80/20/4/1. [Color figure can be viewed in the online issue, which is available at www.interscience.wiley.com.]

Scheme 1 shows a proposed mechanism for the chemical reactions that occur in PA6/EPDM-*g*-MA/OMMT/GMA composites during melt extrusion, which is based on the morphology, FTIR, and Molau test results discussed previously. The epoxy groups of GMA can react with both the amine and carboxylic acid groups of PA6, as shown in Scheme 1(a,b). The resultant compound contains a secondary hydroxyl group that can undergo further reactions. It can react with the MA groups of EPDM-*g*-MA, leading to a copolymer located at the interface and enhancing interfacial adhesion between PA6 and EPDM-*g*-MA, as shown in Scheme 1(c). The amine end groups of PA6 can also react with MA groups of EPDM-*g*-MA to form a copolymer to promote the compatibility of the two phases, as shown in Scheme 1(d).

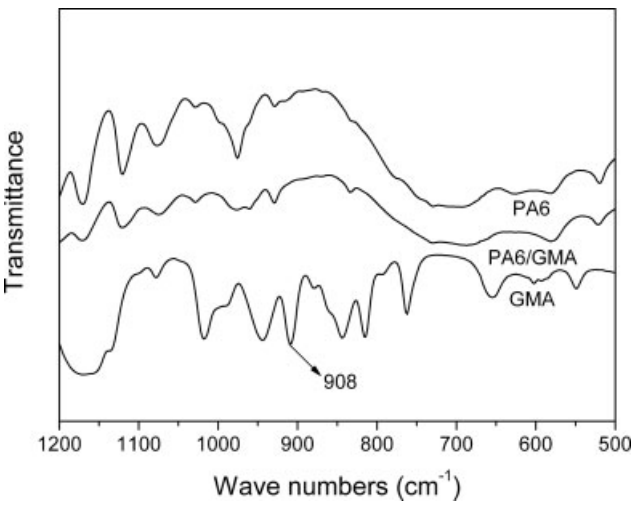

Figure 3 FTIR spectra of PA6, PA6/GMA, and GMA.

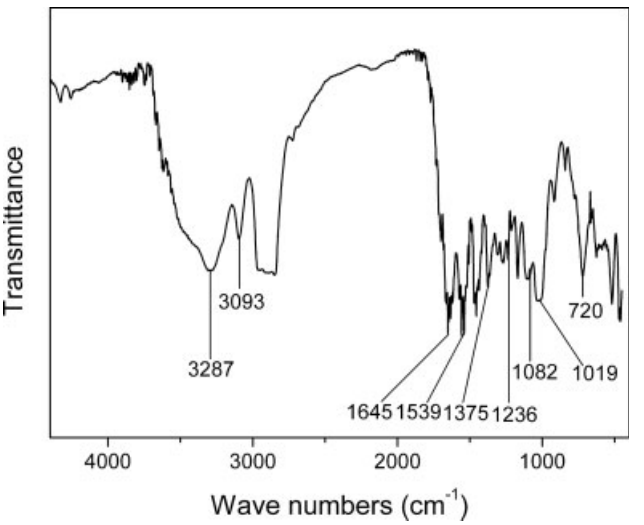

Figure 4 FTIR spectrum of the insoluble fraction of PA6/EPDM-*g*-MA/OMMT/GMA (80/20/4/1) in formic acid.

Dynamic mechanical properties

To further investigate the role of GMA and OMMT, the dynamic mechanical properties of PA6/EPDM-*g*-MA/OMMT composites with and without GMA were investigated. The storage modulus and tan δ were plotted versus the temperature and are shown in Figure 5. The storage modulus significantly increased after the incorporation of 4 phr OMMT, especially in a high temperature range, and changed slightly with the addition of 1 phr GMA. This is consistent with the results for the mechanical properties (see Table I). Figure 5(b) shows the effect of OMMT and GMA on tan δ. Two main peaks were observed around −30 and 57°C, which were related to the glass-transition temperature (T_g) values of EPDM-*g*-

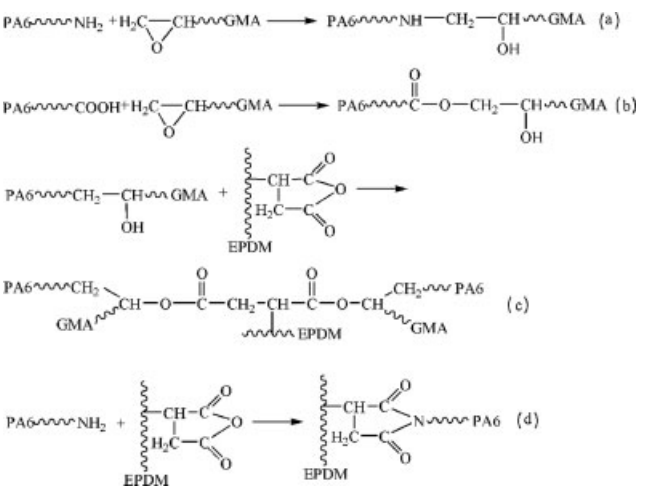

Scheme 1 Proposed reaction mechanism occurring in the PA6/EPDM-*g*-MA/OMMT/GMA composites during melt extrusion.

TABLE III
Tan δ Results for the PA6/EPDM-*g*-MA/OMMT Composites (Prepared by Method N1) with and Without GMA

PA6/EPDM-*g*-MA/OMMT/GMA	Peak 1 (°C)	Tan δ	Peak 2 (°C)	Tan δ
80/20/0/0	−30.9	0.042	56.6	0.115
80/20/1/0	−28.7	0.037	53.9	0.105
80/20/4/0	−35.7	0.037	57.1	0.091
80/20/4/1	−30.5	0.037	57.4	0.091

MA and PA6, respectively. The peak values are listed in Table III. In addition, a prominent relaxation peak below T_g, which is associated with local modes of PA6 main-chain motion, was seen at about −60°C.[26] The data in Table III show that the peak value of tan δ decreased with the addition of OMMT and that the peak position of tan δ varied with the OMMT contents. The incorporation of 1 phr OMMT into PA6/EPDM-*g*-MA blends reduced T_g of PA6 and increased T_g of EPDM-*g*-MA in comparison with PA6/EPDM-*g*-MA blends. However, the reverse trend was observed with the addition of 4 phr OMMT. This phenomenon is different from the results reported in ref. 21, in which the T_g values of polycarbonate and poly(styrene-*co*-acrylonitrile) shifted closer toward each other with an increase in the OMMT content; this means that the compatibility between polycarbonate and poly(styrene-*co*-acrylonitrile) was improved by OMMT. In the PA6/EPDM-*g*-MA/OMMT composites, OMMT might play two competitive roles. On the one hand, *in situ* grafts are proposed to occur on the clay surface during the melt-compounding process, and the formed grafts mainly exist at the interfaces between PA6 and EPDM-*g*-MA phases, which can have the same function as block copolymers, effectively reducing the interfacial tension and the domain size.[21] In this case, OMMT mainly acts as a compatibilizer for the composite. On the other hand, OMMT weakens the interfacial adhesion between PA6 and EPDM-*g*-MA because the layers can shield the interactions of the two phases.[8–11,14–16] Dynamic mechanical analysis is known to be sensitive to the detection of transitions and disturbances caused by chemical reactions and interactions between the phases of reactive blends.[27,28] The T_g values of two phases of polymer blends are known to shift toward each other if they are partially compatible. In our case, the T_g values of PA6 and EPDM-*g*-MA shifted to each other after the addition of 1 phr OMMT, and this means that the compatibility between these two phases was improved. Conversely, the T_g values of PA6 and EPDM-*g*-MA shifted to a reversed direction in the presence of 4 phr OMMT, and this means that a high OMMT loading weakened the interactions between PA6 and EPDM-*g*-MA. As shown in Table III, the tan δ peak of EPDM-*g*-MA in the PA6/EPDM-*g*-MA/OMMT (80/20/4) composite shifted from −35.7 to −30.5°C, and the T_g values of the two phases shifted closer toward each other after the addition of 1 phr GMA. The shift in T_g (by up to 5.2°C in the case of the GMA-modified PA6/EPDM-*g*-MA/OMMT composite) indicated that GMA could enhance the compatibility between the PA6 and EPDM-*g*-MA phases of the composite (80/20/4). It should be noted that the results of dynamic

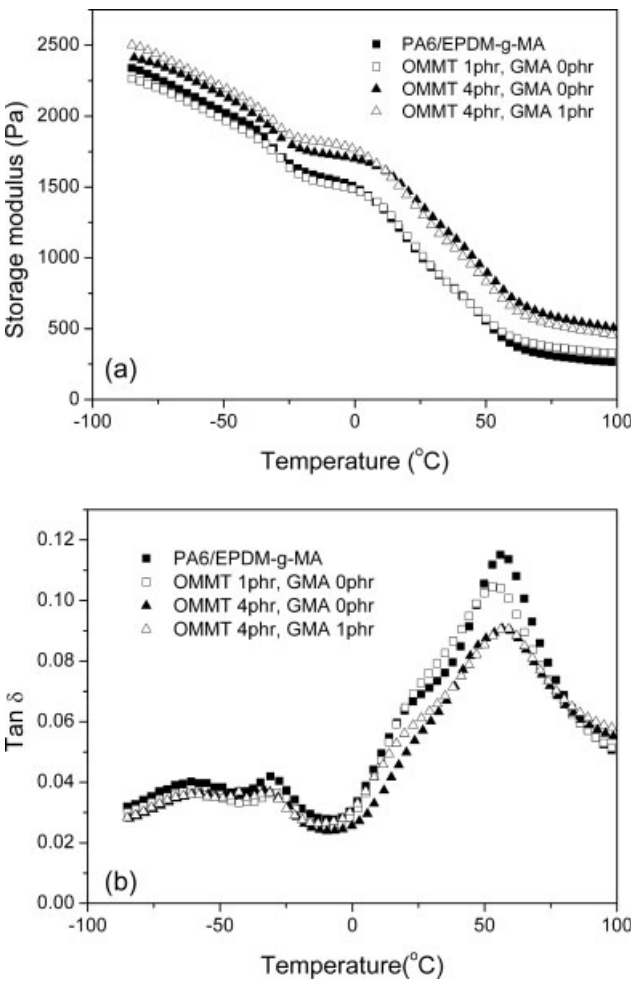

Figure 5 (a) Storage modulus–temperature and (b) tan δ–temperature curves of the PA6/EPDM-*g*-MA/OMMT composites (prepared by method N1) with and without GMA.

mechanical thermal analysis were well supported by the results of FESEM.

Crystal structure and crystallization

PA6 has two different crystalline forms, namely, α and γ.[29] The α form consists of an all-trans chain conformation, and the hydrogen bonds are formed between adjacent antiparallel chains. The γ form consists of twisted chains, which allow hydrogen bonds to form between parallel chains. The formation of these two forms is influenced by the crystallization conditions and the presence of fillers. Figure 6 shows the XRD data for PA6 and the prepared composites in the 2θ range of 1–35°. All samples exhibited a peak at 2θ = 21.2° and a peak at 2θ = 10.7°, which are characteristic of the γ-form structure.[30] Neat PA6 exhibited another two weak peaks at 2θ values of 20.1 and 23.5°, which corresponded to the peaks of the α form. After the addition of OMMT to PA6 and PA6/EPDM-*g*-MA, the two peaks at 2θ = 20.1° and 2θ = 23.5° became weaker. This occurred because OMMT limits the mobility of polymer chains, and this favors the crystallization of γ forms of PA6.[15] The addition of GMA did not change the crystalline forms of PA6 obviously.

Figures 7 and 8 show the differential scanning calorimetry (DSC) cooling and reheating melt thermograms of PA6 and PA6 composites, respectively. The representative thermal data of the samples from the DSC thermograms are listed in Table IV. T_c of neat PA6 was around 190°C, and it shifted to 186–188°C after the addition of OMMT and/or EPDM-*g*-MA. According to the XRD results (Fig. 6), the decrease in T_c can be mainly attributed to the development of γ-form crystals in PA6. T_c shifted to an even lower temperature, approximately 183–184°C, after the addition of 1 phr GMA, and this was due to the limitation of the chain mobility caused by the reactions between PA6, EPDM-*g*-MA, and GMA. T_{onset} is the temperature at the intercept of the tangents at the baseline and high-temperature side of the exotherm. $T_{onset} - T_c$ can be used to indicate the crystallization rate. As shown in Table IV, the $T_{onset} - T_c$ values of the PA6 and PA6/EPDM-*g*-MA blend are quite close to each other. The addition of OMMT or GMA increased the $T_{onset} - T_c$ value, which corresponded to the reduction of the crystallization rate of the PA6 matrix. For all samples, two major melting peaks existed around 212–215 and 219–221°C. According to the reports,[31,32] the high melting temperature (T_{m1}) shoulder is associated with the α-form crystals. The low melting temperature (T_{m2}) corresponds to the T_m values of the γ-form crystals.

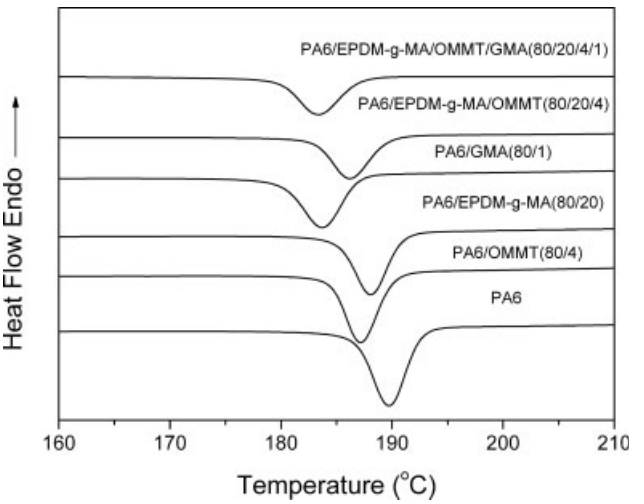

Figure 7 Nonisothermal crystallization curves of the composites (prepared by method N1) at a rate of 10°C/min.

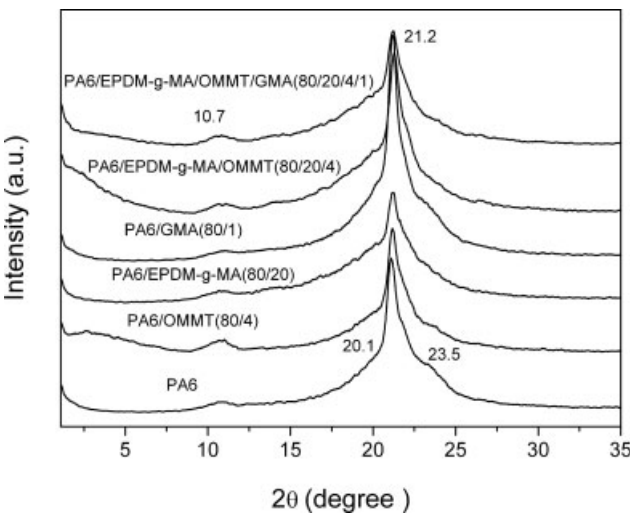

Figure 6 XRD patterns of PA6 and the prepared composites (prepared by method N1).

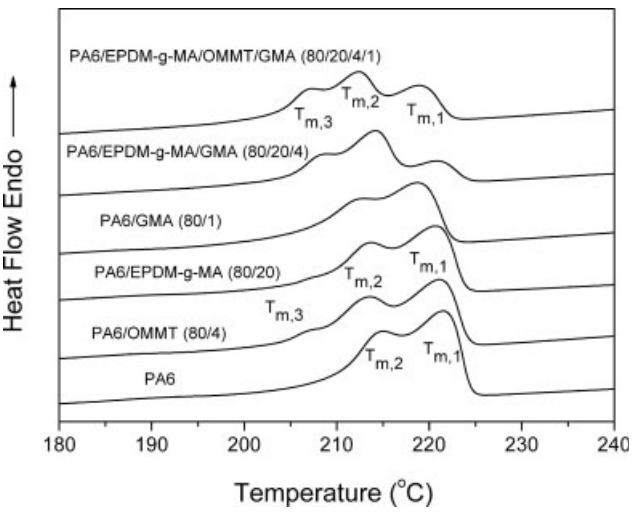

Figure 8 DSC reheating melting curves of the composites (prepared by method N1) at a rate of 10°C/min.

TABLE IV
Thermal Analysis Data Obtained from DSC

Sample	T_c (°C)	$T_{onset} - T_c$ (°C)	T_{m1} (°C)	T_{m2} (°C)	X_c (%)
PA6	189.7	2.9	221.7	215.0	30.5
PA6/OMMT (80/4)	187.3	3.0	221.1	213.6	27.4
PA6/EPDM-*g*-MA (80/20)	188.2	2.8	220.8	213.7	25.3
PA6/GMA (80/1)	183.8	3.1	218.8	213.0	22.6
PA6/EPDM-*g*-MA/OMMT (80/20/4)	186.1	3.5	220.9	214.3	22.8
PA6/EPDM-*g*-MA/OMMT/GMA (80/20/4/1)	183.3	3.7	218.9	212.4	22.1

Besides, a lower melting temperature shoulder (T_{m3}) was observed, as shown in Figure 8, and it was believed to belong to the less stable α-form crystals.[12] It is evident that the T_m and crystallinity degree (X_c) values of PA6 decreased with the addition of OMMT and/or EPDM-*g*-MA. The addition of 1 phr GMA shifted T_m and X_c to lower values. Therefore, both OMMT and GMA retarded the crystallization of PA6.

Oscillatory rheological analysis

Figure 9 shows double logarithmic plots of η*, G', and G'' as functions of the angular frequency (ω) for PA6/EPDM-*g*-MA/OMMT composites at 240°C. As shown in Figure 9(a), all samples exhibited shear-thinning behavior with increasing frequencies, and this indicated the pseudoplastic nature of the samples. The relationships of η*, G', and G'' as a function of ω for the PA6/EPDM-*g*-MA blend were quite similar to those of the PA6/EPDM-*g*-MA/OMMT composite with a low OMMT content (1 phr), although the values of η*, G', and G'' of the composite increased in the low frequency range and decreased in the high frequency range after the addition of 4 phr OMMT, as shown in Figure 9(a–c). It was proposed that as the OMMT content increased, the silicate layers of OMMT could form a percolated network superstructure in the polymer matrix,[33] which may have caused the high η*, G', and G'' values at low shearing rates with the OMMT concentration of 4 phr. However, this percolated network was broken under high shearing forces with an orientation of OMMT layers along the shearing direction, and the degradation of organic molecules of OMMT could stimulate the degradation of PA6;[34] this led to a reduction of the η*, G', and G'' values.

The addition of 1 phr GMA further increased η* significantly, and this was due to the chemical reactions between the amine and carboxylic acid end groups of PA6, the anhydride groups of EPDM-*g*-MA, and the epoxy groups of GMA, as proposed in Scheme 1. Moreover, higher G' and G'' values and more obvious solid-like behavior of the PA6/EPDM-*g*-MA/OMMT composites with 1 phr GMA were observed in comparison with the composite without GMA.

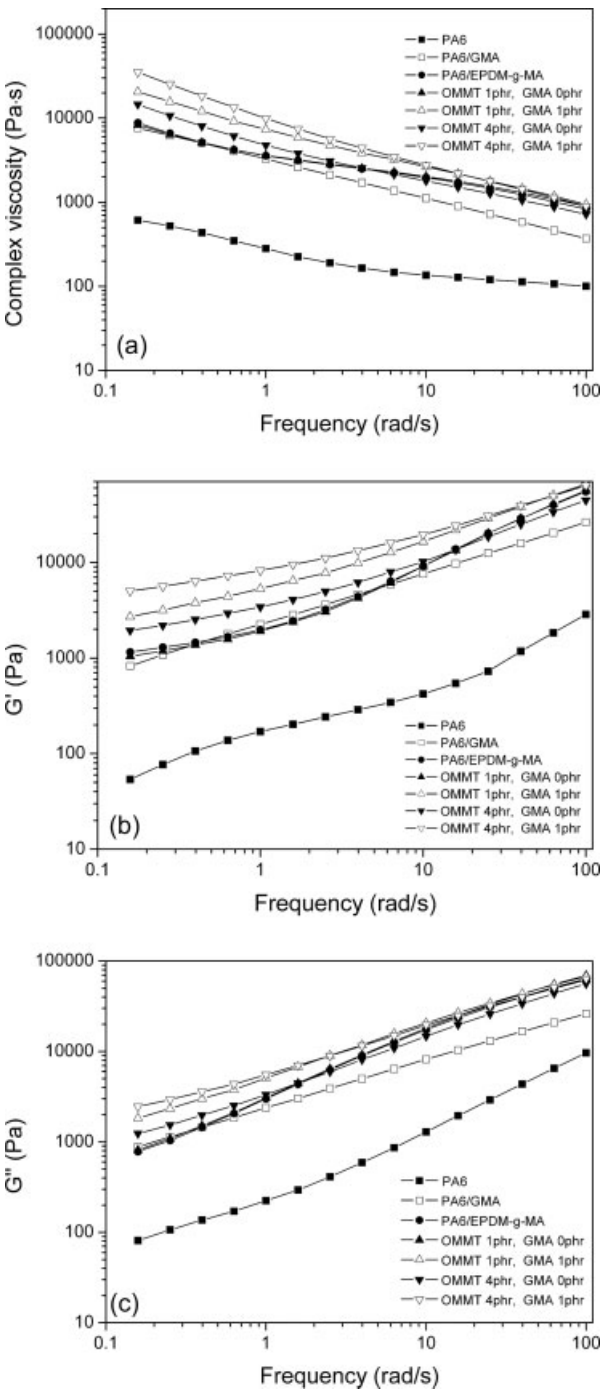

Figure 9 (a) η*–ω, (b) G'–ω, and (c) G''–ω curves for the PA6, PA6/GMA, and PA6/EPDM-*g*-MA/OMMT composites (prepared by method N1) at 240°C.

CONCLUSIONS

The blending sequence could play an important role in determining the mechanical properties of PA6/EPDM-*g*-MA/OMMT (80/20/4) composites. The composite prepared by N1 exhibited much lower impact strength than the composite prepared via a method in which PA6 and OMMT were preblended and then blended with EPDM-*g*-MA (N2). However, satisfactorily balanced mechanical properties of the composite (N1) could be achieved in the presence of GMA. GMA could improve the interfacial interactions between PA6 and EPDM-*g*-MA, as proved by the results of FTIR and Molau testing. OMMT could improve the compatibility between PA6 and EPDM-*g*-MA at low contents but weakened the interfacial interaction at high contents for the composite (N1). Both GMA and OMMT retarded the crystallization of PA6 and influenced the rheological properties of the ternary composites.

The authors thank all the research staff of the Technical Center of the School of Chemistry and Chemical Technology at Shanghai Jiao tong University for the characterization and mechanical testing.

References

1. Okada, O.; Keskkula, H.; Paul, D. R. Polymer 2001, 42, 8715.
2. Wu, S. J Appl Polym Sci 1988, 35, 549.
3. Okada, O.; Keskkula, H.; Paul, D. R. Polymer 2000, 41, 8061.
4. Huang, J. J.; Keskkula, H.; Paul, D. R. Polymer 2006, 47, 624.
5. Xie, X.-L.; Yu, Z.-Z.; Zhang, Q.-X.; Zhang, G.-W.; Mai, Y.-W. J Polym Sci Part B: Polym Phys 2007, 45, 1448.
6. Laura, D. M.; Keskkula, H.; Barlow, J. W.; Paul, D. R. Polymer 2001, 42, 6161.
7. Baldi, F.; Bignotti, F.; Tieghi, G.; Riccò, T. J Appl Polym Sci 2006, 99, 3406.
8. Dasari, A.; Yu, Z.-Z.; Mai, Y.-W. Polymer 2005, 46, 5986.
9. Wang, K.; Wang, C.; Li, J.; Su, J.; Zhang, Q.; Du, R.; Fu, Q. Polymer 2007, 48, 2144.
10. Dasari, A.; Yu, Z.-Z.; Mai, Y.-W. Acta Mater 2007, 55, 635.
11. Dasari, A.; Yu, Z.-Z.; Yang, M.; Zhang, Q.-X.; Xie, X.-L.; Mai, Y.-W. Compos Sci Technol 2006, 66, 3097.
12. Chiu, F.-C.; Lai, S.-M.; Chen, Y.-L.; Lee, T.-H. Polymer 2005, 46, 11600.
13. Ahn, Y.-C.; Paul, D. R. Polymer 2006, 47, 2830.
14. González, I.; Eguiazábal, J. I.; Nazábal, J. Compos Sci Technol 2006, 66, 1833.
15. González, I.; Eguiazábal, J. I.; Nazábal, J. Eur Polym J 2006, 42, 2905.
16. González, I.; Eguiazábal, J. I.; Nazábal, J. J Polym Sci Part B: Polym Phys 2005, 43, 3611.
17. Yu, Z.-Z.; Ou, Y.-C.; Hu, G.-H. J Appl Polym Sci 1998, 69, 1711.
18. Jannerfeldt, G.; Boogh, L.; Månson, J.-A. E. Polymer 2000, 41, 7627.
19. Molau, G. E. J Polym Sci Part A: Gen Pap 1965, 3, 4235.
20. Russo, P.; Acierno, D.; Di, M. L.; Demma, G. Eur Polym J 1999, 35, 1261.
21. Si, M.; Araki, T.; Ade, H.; Kilcoyne, A. L. D.; Fisher, R.; Sokolov, J. C.; Rafailovich, M. H. Macromolecules 2006, 39, 4793.
22. Khatua, B. B.; Lee, D. J.; Kim, H. Y.; Kim, J. K. Macromolecules 2004, 37, 2454.
23. Qin, H.; Su, Q.; Zhang, S.; Zhao, B.; Yang, M. Polymer 2003, 44, 7533.
24. Wan, T.; Clifford, M. J.; Gao, F.; Bailey, A. S.; Gregory, D. H.; Somsunan, R. Polymer 2005, 46, 6429.
25. Wu, Q.; Liu, X.; Berglund, L. A. Polymer 2002, 43, 2445.
26. Chow, W. S.; Ishak, Z. A. M.; Karger-Kocsis, J.; Apostolov, A. A.; Ishiaku, U.S. Polymer 2003, 44, 7427.
27. Al-Malaika, S.; Kong, W. Polymer 2005, 46, 209.
28. Singh, D.; Malhotra, V. P.; Vats, J. L. J Appl Polym Sci 1999, 71, 1959.
29. Ramesh, C.; Bhoje Gowd, E. Macromolecules 2001, 34, 3308.
30. Fornes, T. D.; Paul, D. R. Macromolecules 2004, 37, 7698.
31. Liu, L.; Qi, Z.; Zhu, X. J Appl Polym Sci 1999, 71, 1133.
32. Liu, T. X.; Liu, Z. H.; Ma, K. X.; Shen, L.; Zeng, K. Y.; He, C. B. Compos Sci Technol 2003, 63, 331.
33. Tung, J.; Gupta, R. K.; Simon, G. P.; Edward, G. H.; Bhattacharya, S. N. Polymer 2005, 46, 10405.
34. Fornes, T. D.; Yoon, P. J.; Keskkula, H.; Paul, D. R. Polymer 2003, 44, 7545.